Journal of Magnetism and Magnetic Materials 586 (2023) 171163

Contents lists available at ScienceDirect

Journal of Magnetism and Magnetic Materials

journal homepage: www.elsevier.com/locate/jmmm

Research article

Orbital-selective altermagnetism and correlation-enhanced spin-splitting in strongly-correlated transition metal oxides

Giuseppe Cuono *, Raghottam M. Sattigeri, Jan Skolimowski, Carmine Autieri

International Research Centre Magtop, Institute of Physics, Polish Academy of Sciences, Aleja Lotników 32/46, PL-02668 Warsaw, Poland

ARTICLE INFO

Keywords:
Altermagnetism
Strongly correlated systems
Density functional theory
Perovskites

ABSTRACT

We investigate the altermagnetic properties of strongly-correlated transition metal oxides considering the family of the quasi two-dimensional A_2BO_4 and three-dimensional ABO_3. As a test study, we analyze the Mott insulators Ca_2RuO_4 and YVO_3. In both cases, the orbital physics is extremely relevant in the t_{2g} subsector with the presence of an orbital-selective Mott physics in the first case and of a robust orbital-order in the second case. Using *first-principles* calculations, we show the presence of an orbital-selective altermagnetism in the case of Ca_2RuO_4. In the case of YVO_3, we study the altermagnetism as a function of the magnetic ordering and of the Coulomb repulsion U. We find that the altermagnetism is present in all magnetic orders with the symmetries of the Brillouin zone depending on the magnetic order. Finally, the Coulomb repulsion enhances the non-relativistic spin-splitting making the strongly-correlated systems an exciting playground for the study of the altermagnetism.

1. Introduction

The spin splitting of the energy bands typical for the ferromagnetic and ferrimagnetic configurations was also found in magnetically ordered compounds with zero net magnetization. These compounds with compensated magnetic moments in the real space but with spin-polarization order in the reciprocal space are named altermagnets [1,2]. As a consequence of the non-relativistic spin splitting [3,4], the altermagnetic systems exhibit an anomalous Hall effect even without a ferromagnetic order in the real space [5], as for example in MnTe [6]. This happens when the opposite-spin sublattices are connected by roto-translations and not by inversion or translation mechanisms. These conditions are satisfied in many antiferromagnetic systems with antiferro orbital-order [7]. The magnetic space groups are classified into four types, depending on the relation to the parent crystallographic space group [8]. In a recent work, it was shown that the altermagnetism can be found in the type-I and type-III magnetic space groups [9]. Several transition metal oxides [9,10] and rare-earth compounds [11] have been shown to exhibit altermagnetism. We have shown that altermagnetism survives selectively on the surface states [12] and has an interplay with the non-symmorphic symmetries [13–15]. The altermagnets can also be used in applications like spintronics [16], for highly efficient spin-current generation [17], to produce giant and tunneling magnetoresistance [18] and can be useful in spincaloritronics [19] and in Josephson junctions [20].

In the strongly-correlated transition metal oxides, the interplay between magnetism and orbital physics plays an important role [21]. Looking for altermagnetism with large non-relativistic spin-splitting, we need to search for systems with strong orbital order. The orbital-order could be in the e_g subsector [22–24] or in the t_{2g} subsector. In this paper, we focus on compounds with orbital order in the latter. To investigate the altermagnetism in transition metal oxides, we choose two systems belonging to the two major classes of oxide perovskites: the quasi two-dimensional A_2BO_4 and three-dimensional ABO_3. Regarding the quasi two-dimensional case, we investigate Ca_2RuO_4 while for the three-dimensional case, we study YVO_3. In both cases, the interplay between the electronic correlation and the orbital physics is extremely relevant in the t_{2g} subsector, which dominates the low energy physics. Ca_2RuO_4 is an antiferromagnetic Mott insulator with orbital-selective Mott physics [25–27] and spin–orbital correlation driven negative thermal expansion [28]. Recently, the metal–insulator transition induced by electric current or electric field was deeply investigated in this compound [29]. The large family of vanadate oxides AVO_3 (A = La, Y, ...) was intensively studied for the interplay between orbital and magnetic orders and the metal–insulator transition present in this material class [30–34]. Recently, a member of the vanadates family has been predicted to be a rare Kugel–Khomskii system where a purely electronic mechanism can drive the orbital-order via the superexchange [35]. We decide to investigate YVO_3 which presents the largest distortions and

* Corresponding author.
E-mail addresses: gcuono@magtop.ifpan.edu.pl (G. Cuono), autieri@magtop.ifpan.edu.pl (C. Autieri).

https://doi.org/10.1016/j.jmmm.2023.171163
Received 22 May 2023; Received in revised form 9 August 2023; Accepted 21 August 2023
Available online 22 August 2023
0304-8853/© 2023 The Author(s). Published by Elsevier B.V. This is an open access article under the CC BY license (http://creativecommons.org/licenses/by/4.0/).

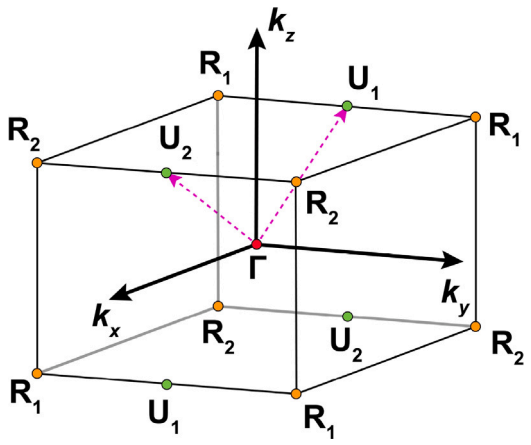


Fig. 1. Symmetries of the irreducible Brillouin zone for the orthorhombic Ca_2RuO_4 (space group Pbca no. 61). In our notation, the high-symmetry points with the subscript 1 and 2 show altermagnetism along the path towards the Γ point. The position of the high-symmetry k-points U_1, U_2, R_1 and R_2 are highlighted in green and orange. The dashed magenta line indicates the high-symmetry path $U_1 - \Gamma$-U_2 which is one of the possible paths to show the altermagnetism in this magnetic space group.

therefore the most robust orbital-order among the members of this family.

Using first principle calculations, we demonstrate the presence of altermagnetism in both Ca_2RuO_4 and YVO_3. We discover an orbital-selective altermagnetism in Ca_2RuO_4 and we report the evolution of the altermagnetism as a function of the magnetic order and Coulomb repulsion in the vanadates family.

The paper is organized as follows: in the second Section, we illustrate the computational details and symmetries of the systems. In the third Section, we study the orbital-selective altermagnetism in quasi two-dimensional Ca_2RuO_4 while in the fourth Section, we show our results for the correlation-enhanced non-relativistic spin-splitting in YVO_3. Finally, we draw our conclusions.

2. Computational details and symmetries

We performed density functional theory calculations by using the VASP package [36–38]. As an exchange–correlation functional, the generalized gradient approximation (GGA) of Perdew, Burke, and Ernzerhof has been adopted [39]. All the calculations have been done without considering relativistic effects. For the Ca_2RuO_4, we have investigated the so-called short phase S-Pbca with space group no. 61. A plane-wave energy cut-off of 480 eV has been used. We have minimized the total energy to be less than 1×10^{-5} eV. The calculations have been performed with $11 \times 11 \times 4$ k-points. We have used the experimental lattice constants a = 5.3945 Å, b = 5.5999 Å, c = 11.7653 Å in the S-Pbca phase. We have employed a Coulomb repulsion of U = 3 eV on the d-orbitals of the Ru-4d [40], while for the Hund coupling J_H = 0.15 U has been employed, in agreement with the literature for 4d/5d electrons [41]. In previous literature, a value of the Coulomb repulsion smaller than 1 eV was used in bulk ruthenates [42,43]. Moreover, in the insulating phase the screening effect is reduced and the value of the Coulomb repulsion is higher. This computational set of parameters was already used in a previous paper [44]. Within this setup, the magnetic moment is $1.4\mu_B$ per Ru atom as expected for the typical magnetic configuration in Ca_2RuO_4 with $4dt^3_{2g}\uparrow t^1_{2g}\downarrow$. For the YVO_3, a plane-wave energy cut-off of 400 eV has been used. We mapped the momentum space with an $8 \times 8 \times 6$ k-mesh centered at Γ with 100 independent k-points in the Brillouin zone (BZ). We have used the Coulomb repulsion U on the 3d-V orbitals with the Hund coupling J_H=0.15U. We have scanned U between 0 and 5 eV with the best value being around U = 3 eV, as suggested by previous works, where it was found that this value reproduces the experimental band gap [45]. The magnetic moment is 1.8 μ_B per V atom with the magnetic configuration $3dt^2_{2g}\uparrow$. The crystal structure is the Pbnm with space group no. 62 observed upon cooling below 77 K. We have used the experimental positions and the lattice constants reported at 5 K [46].

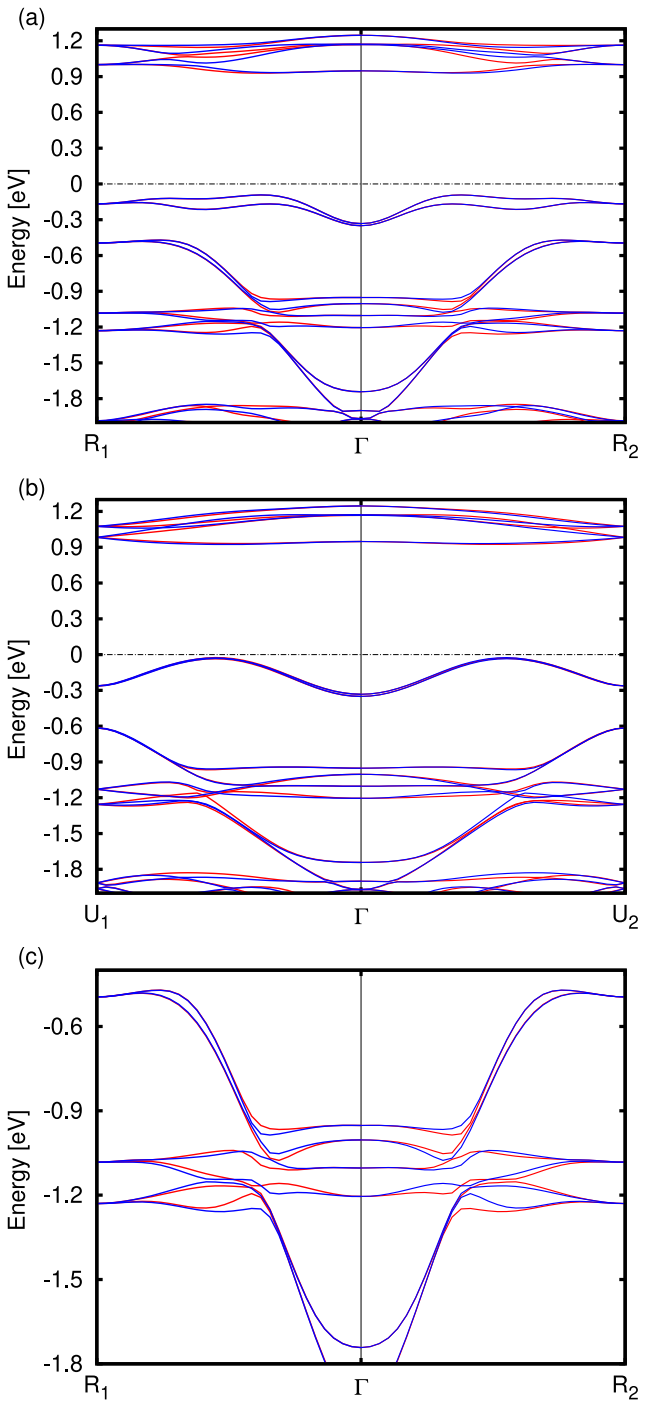


Fig. 2. (a) Band structure of Ca_2RuO_4 along the high-symmetry positions $R_1 - \Gamma$-R_2. (b) Band structure of Ca_2RuO_4 along the high-symmetry positions $U_1 - \Gamma$-U_2. (c) Magnification of the band structure along the $R_1 - \Gamma$-R_2 k-path with energy between −1.8 and −0.4 eV. Blue and red lines represent the spin-up and spin-down channels, respectively.

3. Orbital-selective altermagnetism in Ca_2RuO_4

The symmetries of the BZ for the antiferromagnetic phase of Ca_2RuO_4 are reported in Fig. 1. With the subscripts 1 and 2, we indicate the two points in the k-space that have opposite non-relativistic spin-splitting. We plot the non-relativistic band structure of Ca_2RuO_4 in Fig. 2 along two different k-paths $R_1 - \Gamma$-R_2 (top panel) and $U_1 - \Gamma$-U_2 (middle panel). In Fig. 2(c) we show a magnification of the band structure along $R_1 - \Gamma$-R_2. These k-paths represent the regions of the k-space where the altermagnetic spin-splitting is maximum, but it survives in all the BZ except for the high-symmetry directions where one of the k-component is zero or on the zone boundaries of the BZ. The band structures are composed of two sets of bands. The first set is composed of 4 weekly dispersive bands at around −1 eV and 4 weekly dispersive bands at around +1 eV with respect to the Fermi level. The other set is more dispersive and it is composed of 2 bands in the top of the valence and the other 2 bands that have a bandwidth from −0.5 to −2.0 eV. From previous literature [44,47,48], we know that the less dispersive bands at around −1 eV and +1 eV have mainly d_{xz}/d_{yz} character, while the others are mainly d_{xy}. The lowest d_{xy} band has a bandwidth between −0.5 and −2.0 eV while it hybridizes with the majority d_{xz}/d_{yz} bands around −1 eV. In both k-paths, we observe the presence of non-relativistic spin-splitting in the d_{xz}/d_{yz} bands while the splitting is suppressed in the d_{xy} bands. This orbital-selective altermagnetism cannot be explained only with orbital-dependent spin-splitting. In the antiferromagnets, at each lattice site there are a majority and a minority spin channel. The altermagnetic spin-splitting does depend on the spin-splitting between the majority (maj) and minority (min) spin-channels E^{min}-E^{maj}. This quantity shows strong orbital dependence in Ca_2RuO_4. At the Γ point, $E^{min}_{d_{xy}}$-$E^{maj}_{d_{xy}}$= 1.6 eV while $E^{min}_{d_{xz}/d_{yz}}$-$E^{maj}_{d_{xz}/d_{yz}}$ = 2.2 eV. Nonetheless, this difference is not enough to explain this large orbital-selective effect. We show that this scenario is made possible by the quasi-two-dimensionality of a system with t_{2g} electrons. The d_{xy} orbitals have negligible hopping parameters between the layers, therefore we can assume that the d_{xy} bands are two-dimensional [49,50]. Therefore, we have a mirror plane that produces an approximated mirror symmetry and suppresses the altermagnetism as we can see in the schematic picture Fig. 3(a). However, the d_{xz}/d_{yz} orbitals are 3D and this plane is not a mirror anymore when we go in 3D as we can see in Fig. 3(b). In Fig. 3(c,d), we report the top view of the d_{xz}/d_{yz} orbitals. We observe that there is no mirror for the 3D orbitals but there is a rotation of 90 degrees that map the d_{xz}/d_{yz} spin-up in the d_{yz}/d_{xz} spin-down and vice-versa realizing the altermagnetism.

The AHE was deeply investigated in ferromagnetic ruthenates oxides and its interfaces for the tunable properties deriving from the Berry phase and for the presence of humps [51–55]. Due to the orbital selective altermagnetism, we obtain that the AHE can be measured in Ca_2RuO_4 just in n-doped samples while the highest valence bands show no sizeable altermagnetism.

4. Correlation effects on the altermagnetic properties of YVO_3

Now we shift our attention to the second class of oxide perovskites that we want to investigate, namely the three-dimensional ABO_3. We analyze the altermagnetism in YVO_3 as a function of the magnetic order. The magnetic orders usually investigated in transition-metal perovskite ABO_3 with four formula units in the unit cell are A-type, C-type and G-type, shown in Fig. 4 together with the magnetic space group numbers and types [56]. The band gaps of the three different magnetic orders at U = 3 eV are 1.39 eV, 1.48 eV and 1.69 eV, respectively. The altermagnetism is present in all magnetic orders and this outcome is not granted by the space group No. 62. Indeed, by changing the magnetic configuration, the system changes the magnetic space group. Since YVO_3 stays altermagnetic in all magnetic configurations, it means that all the magnetic space groups of the different configurations belong to types I and III. The magnetic space groups for A-type are 62.448, 62.447 and 62.441 for the Néel vector along x, y and z, respectively. The C-type configurations belong to the space groups 62.446, 62.441 and 62.447 for the Néel vector along x, y and z, respectively, while for the G-type configuration, the magnetic space groups are 62.441, 62.446 and 62.448 for the Néel vector along x, y and z, respectively. The space group 62.441 belongs to Type-I while all others belong to the type-III magnetic space groups. In other compounds with space group No. 62 but different crystal structures and magnetic space group, the altermagnetism was observed just in one of the magnetic orders [15]. In Fig. 5, we show the way how symmetries of the BZ evolve which is not straightforward as a function of the magnetic order. For the C-type magnetic order, we have a checkerboard pattern of R_1 and R_2 while no altermagnetism is present neither along Γ-U nor Γ-T as shown in Fig. 5(b). For the A-type and G-type, we have consecutive R_1 and R_2 along the k_x and k_y axis, respectively. The altermagnetism is present also along the Γ-T and Γ-U paths for the A-type and G-type magnetic orders, respectively. As a consequence, the C-type magnetic order has fewer regions of the k-space where altermagnetism is present. We report in Fig. 6 the band structure along the $R_1 - \Gamma$-R_2 path for the three magnetic orders. Despite the minor region of the k-space with altermagnetism, the C-type is the magnetic order that shows larger non-relativistic spin-splittings. The A-type shows very small non-relativistic spin-splittings, while in the G-type magnetic order we obtain intermediate values for the spin-splittings. It is important to highlight that in the case of YVO_3 we do not have orbital-selective altermagnetism, namely the non relativistic spin splitting is present for all the majority t_{2g} V-bands, as we can see in Fig. 6.

Finally, we report the evolution of the non-relativistic spin-splitting as a function of the Coulomb repulsion for the majority t_{2g} V-orbitals. We consider the midpoint between Γ and R in the momentum space, since the large spin-splitting is zero at Γ and R and it is usually maximum at halfway [1,2]. In more detail, we consider the evolution of the spin-splitting at the vector k = (0.25, 0.25, 0.25) for all the 6 bands of the majority t_{2g} V-orbitals. The results are reported in Fig. 7 for the G-type magnetic order. We indicate with N the highest valence band, and starting from this with N−1, N−2... we go to the lower valence bands and with N+1 to the lowest conduction band and so on. The Coulomb repulsion is uniform over the Brillouin zone, therefore it will

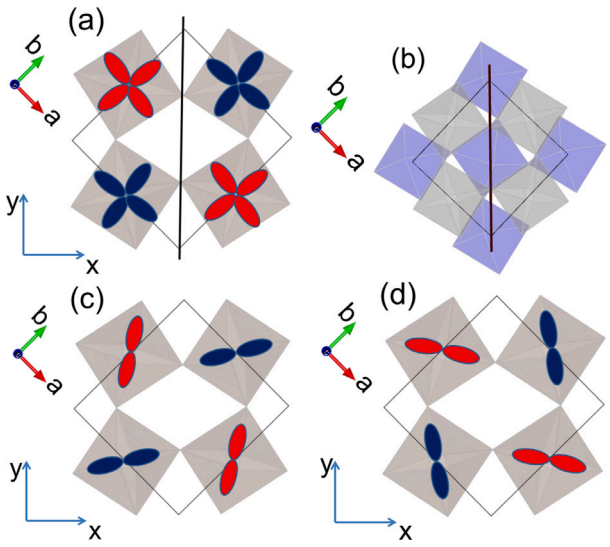


Fig. 3. (a) Schematic top view of the d_{xy} majority electrons in a 2D plane cut by a perpendicular mirror plane in black. (b) The same plane used as a mirror in the 2D case is not a mirror plane anymore in the 3D crystal structure of Ca_2RuO_4. The grey and light blue colors indicate the octahedra in different planes. (c) Schematic top view of d_{xz} spin-up and d_{yz} spin-down majority electrons. (d) Schematic top view of d_{yz} spin-up and d_{xz} spin-down majority electrons. We use the color blue and red for the spin sublattices up and down, respectively.

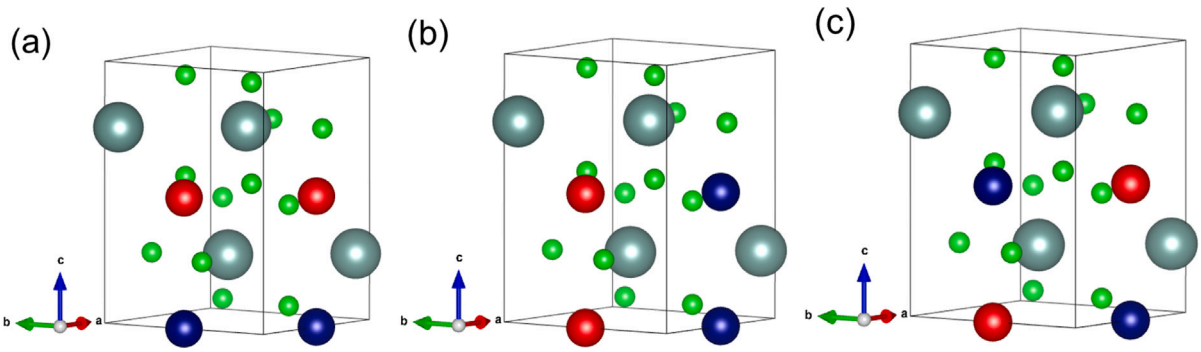


Fig. 4. Crystal structure of YVO_3 for the (a) A-type, (b) C-type and (c) G-type magnetic order in the Pbnm setting. The spheres with colors blue and red represent the V atoms with the opposite spin moments. The grey spheres are the Y atoms, while the green spheres are the O atoms. The magnetic space groups for A-type, C-type and G-type configurations are described in the text.

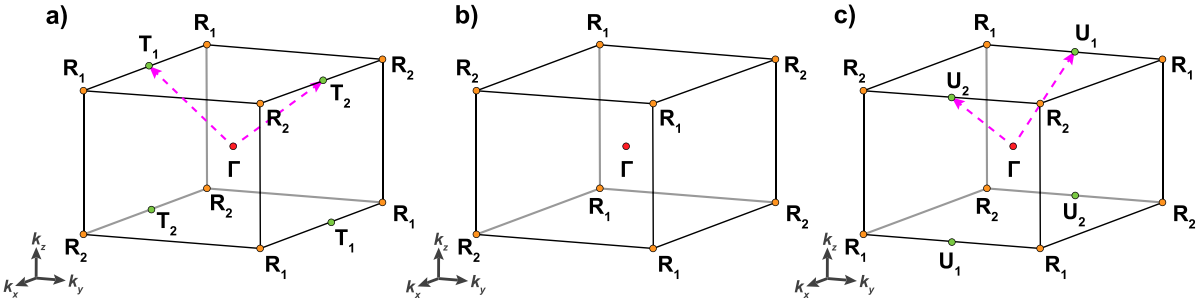


Fig. 5. Symmetries of the Brillouin zone for the (a) A-type, (b) C-type and (c) G-type magnetic order of YVO_3 (space group no. 62) in the Pbnm setting. In our notation, the high-symmetry points with the subscript 1 and 2 show altermagnetism along the path towards the Γ point. The positions of the points R_1 and R_2 evolve as a function of the magnetic order. In A-type and G-type magnetic orders, the k-paths Γ-T and Γ-U show altermagnetic spin-splitting, respectively.

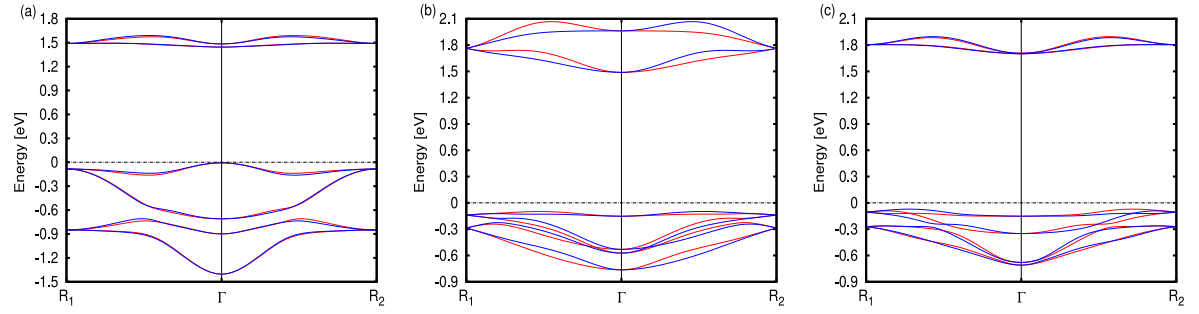


Fig. 6. Spin-splitting along the $R_1 - \Gamma - R_2$ for the majority t_{2g} V-bands of YVO_3 for the (a) A-type, (b) C-type and (c) G-type magnetic order. In these cases, we have used the value of U = 3 eV. The spin-up channel is shown in blue, while the spin-down channel is shown in red.

affect the band structure at all k-points in the same way. The absolute values of the spin-splittings for all six bands are considered at U = 0, if the spin-splitting change sign we use the negative value. From the plot, we conclude that the spin-splitting at U = 0 is relatively small due to the weak electronic dispersion of the strongly-correlated bands. However, the Coulomb repulsion enhances on average the non-relativistic spin-splitting. Indeed, we have a correlation-enhanced non-relativistic spin-splitting up to a factor 4–5 with respect to the initial splitting at U = 0. The motivation for this large increase is the following. The relevant quantity for the altermagnetic spin-splitting is the spin-splitting between minority and majority t_{2g} electrons $E^{min}_{t_{2g}}$-$E^{maj}_{t_{2g}}$, this quantity increases with U. As the splitting between minority and majority increases with U, the altermagnetic spin-splitting on average follows a similar trend. We also report a similar evolution of the non-relativistic spin-splitting as a function of the Coulomb repulsion for the majority t_{2g} V-orbitals for the C-type configuration. The results are shown in Fig. 8. We do not show the evolution of the spin-splitting for the A-type configuration because it is smaller compared to the other cases.

As a weak point of this analysis, in both Ca_2RuO_4 and YVO_3 the non-relativistic spin-splitting is relatively weak despite the strong orbital-order in YVO_3. Therefore, to obtain very large non-relativistic spin-splitting we need both strong orbital-order and large hopping parameters. The latter are usually not present in strongly-correlated systems.

5. Conclusions

Using *first-principles* calculations, we have investigated the altermagnetism in strongly correlated systems with an orbital order in the t_{2g} subsector, choosing two systems belonging to the two major classes of oxide perovskites: the quasi two-dimensional A_2BO_4 and three-dimensional ABO_3. We have found an orbital-selective altermagnetism in quasi 2D Ca_2RuO_4. While the d_{xz}/d_{yz} orbitals are connected only by a roto-translation as requested condition to observe the altermagnetism, the quasi-twodimensionality of the d_{xy} bands allows introducing a mirror plane that strongly suppresses the altermagnetism in the d_{xy} bands. In the YVO_3, the altermagnetism is present in all magnetic configurations. We have shown how the symmetries of Brillouin zone evolve in

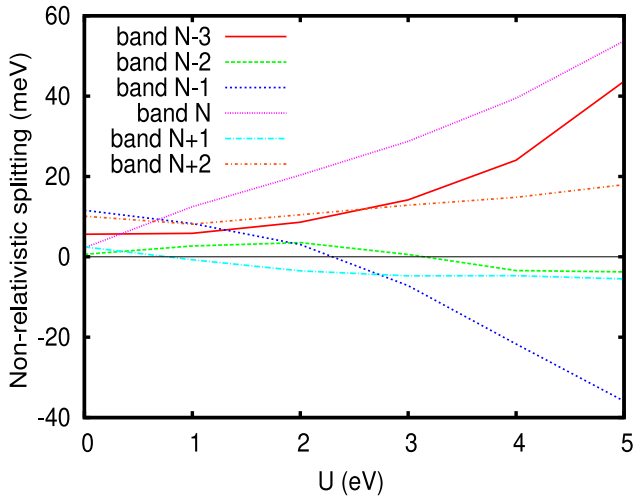


Fig. 7. Evolution of the spin-splitting at the vector k = (0.25, 0.25, 0.25) as a function of the Coulomb repulsion in the G-type order for all 6 bands of the majority t_{2g} V-orbitals. The band number *N* is the highest valence band while the band number N+1 is the lowest conduction band. We considered the absolute value of the splitting at U = 0 and we assume it as negative when the spin-splitting changes sign.

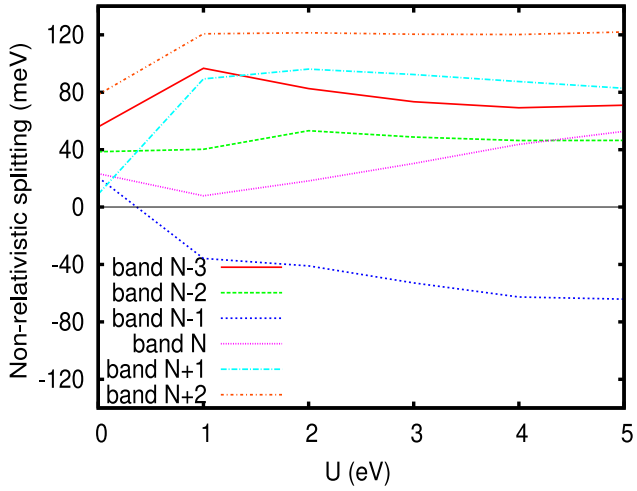


Fig. 8. Evolution of the spin-splitting at the vector k = (0.25, 0.25, 0.25) as a function of the Coulomb repulsion in the C-type order for all 6 bands of the majority t_{2g} V-orbitals. The band number *N* is the highest valence band while the band number N+1 is the lowest conduction band. We considered the absolute value of the splitting at U = 0 and we assume it as negative when the spin-splitting changes sign.

the three-dimensional YVO_3 as a function of the magnetic order. The non-relativistic spin-splitting is larger for the C-type magnetic order. We report that the Coulomb repulsion enhances the non-relativistic spin-splitting making the strongly-correlated system a platform for the research of altermagnetic properties.

Recently, the altermagnetic properties as a function of the magnetic order in perovskites were described in terms of non-interconvertible spin-structure motif pair [57].

CRediT authorship contribution statement

Giuseppe Cuono: Conceptualization, Investigation, Methodology, Data curation, Software, Writing – original draft, Writing – review & editing. **Raghottam M. Sattigeri:** Visualization, Validation, Data curation, Investigation, Writing – review & editing. **Jan Skolimowski:** Investigation, Validation, Writing – review & editing. **Carmine Autieri:** Supervision, Validation, Writing – original draft, Writing – review & editing, Investigation, Methodology, Conceptualization.

Declaration of competing interest

The authors declare that they have no known competing financial interests or personal relationships that could have appeared to influence the work reported in this paper.

Data availability

Data will be made available on request.

Acknowledgments

We thank Tomasz Dietl, Mario Cuoco, Adolfo Avella and Amar Fakhredine for useful discussions. The work is supported by the Foundation for Polish Science through the International Research Agendas program co-financed by the European Union within the Smart Growth Operational Programme (Grant No. MAB/2017/1). J. S. is supported by the National Science Centre (Poland) OPUS 2021/41/B/ST3/04475. We acknowledge the access to the computing facilities of the Interdisciplinary Center of Modeling at the University of Warsaw, Grant G84-0, GB84-1 and GB84-7. We acknowledge the CINECA award under the ISCRA initiative IsC85 "TOPMOST" and IsC93 "RATIO" grant, for the availability of high-performance computing resources and support. We acknowledge the access to the computing facilities of the Poznan Supercomputing and Networking Center Grant No. 609.

References

[1] Libor Šmejkal, Jairo Sinova, Tomas Jungwirth, Emerging research landscape of altermagnetism, Phys. Rev. X 12 (2022) 040501, URL https://link.aps.org/doi/10.1103/PhysRevX.12.040501.

[2] Libor Šmejkal, Jairo Sinova, Tomas Jungwirth, Beyond conventional ferromagnetism and antiferromagnetism: A phase with nonrelativistic spin and crystal rotation symmetry, Phys. Rev. X 12 (2022) 031042, URL https://link.aps.org/doi/10.1103/PhysRevX.12.031042.

[3] Satoru Hayami, Yuki Yanagi, Hiroaki Kusunose, Momentum-dependent spin splitting by collinear antiferromagnetic ordering, J. Phys. Soc. Japan 88 (12) (2019) 123702, http://dx.doi.org/10.7566/JPSJ.88.123702.

[4] Satoru Hayami, Yuki Yanagi, Hiroaki Kusunose, Bottom-up design of spin-split and reshaped electronic band structures in antiferromagnets without spin-orbit coupling: Procedure on the basis of augmented multipoles, Phys. Rev. B 102 (2020) 144441.

[5] Libor Šmejkal, Rafael González-Hernández, T. Jungwirth, J. Sinova, Crystal time-reversal symmetry breaking and spontaneous hall effect in collinear antiferromagnets, Sci. Adv. 6 (23) (2020) eaaz8809.

[6] R.D. Gonzalez Betancourt, J. Zubáč, R. Gonzalez-Hernandez, K. Geishendorf, Z. Šobáň, G. Springholz, K. Olejník, L. Šmejkal, J. Sinova, T. Jungwirth, S.T.B. Goennenwein, A. Thomas, H. Reichlová, J. Železný, D. Kriegner, Spontaneous anomalous hall effect arising from an unconventional compensated magnetic phase in a semiconductor, Phys. Rev. Lett. 130 (2023) 036702.

[7] E. Pavarini, E. Koch, A.I. Lichtenstein, Mechanism for orbital ordering in $KCuF_3$, Phys. Rev. Lett. 101 (2008) 266405.

[8] C. Bradley, A. Cracknell, The Mathematical Theory of Symmetry in Solids: Representation Theory for Point Groups and Space Groups, in: EBSCO ebook academic collection, OUP Oxford, 2010.

[9] Yaqian Guo, Hui Liu, Oleg Janson, Ion Cosma Fulga, Jeroen van den Brink, Jorge I. Facio, Spin-split collinear antiferromagnets: A large-scale ab-initio study, Mater. Today Phys. 32 (2023) 100991.

[10] Xin Chen, Duo Wang, Linyang Li, Biplab Sanyal, Giant spin-splitting and tunable spin-momentum locked transport in room temperature collinear antiferromagnetic semimetallic CrO monolayer, Appl. Phys. Lett. 123 (2) (2023) 022402, arXiv:https://pubs.aip.org/aip/apl/article-pdf/doi/10.1063/5.0147450/18038936/022402_1_5.0147450.pdf.

[11] Giuseppe Cuono, Raghottam M. Sattigeri, Carmine Autieri, Tomasz Dietl, Ab-initio overestimation of the topological region in eu-based compounds, Phys. Rev. B 108 (2023) 075150.

[12] Raghottam M Sattigeri, Giuseppe Cuono, Carmine Autieri, Altermagnetic surface states: towards the observation and utilization of altermagnetism in thin films, interfaces and topological materials, 2023, arXiv:2307.10146[cond-mat.mtrl-sci].

[13] Giuseppe Cuono, Filomena Forte, Mario Cuoco, Rajibul Islam, Jianlin Luo, Canio Noce, Carmine Autieri, Multiple band crossings and Fermi surface topology: Role of double nonsymmorphic symmetries in MnP-type crystal structures, Phys. Rev. Mater. 3 (2019) 095004.

[14] D.J. Campbell, J. Collini, J. Sławińska, C. Autieri, L. Wang, K. Wang, B. Wilfong, Y.S. Eo, P. Neves, D. Graf, E.E. Rodriguez, N.P. Butch, M. Buongiorno Nardelli, J. Paglione, Topologically driven linear magnetoresistance in helimagnetic FeP, npj Quantum Mater. 6 (1) (2021) 38.

[15] Amar Fakhredine, Raghottam M. Sattigeri, Giuseppe Cuono, Carmine Autieri, Interplay between altermagnetism and nonsymmorphic symmetries generating large anomalous hall conductivity by semi-dirac points induced anticrossings, 2023, arXiv:2308.08416[cond-mat.mtrl-sci].

[16] Ding-Fu Shao, Shu-Hui Zhang, Ming Li, Chang-Beom Eom, Evgeny Y. Tsymbal, Spin-neutral currents for spintronics, Nature Commun. 12 (2021).

[17] Rafael González-Hernández, Libor Šmejkal, Karel Výborný, Yuta Yahagi, Jairo Sinova, Tomáš Jungwirth, Jakub Železný, Efficient electrical spin splitter based on nonrelativistic collinear antiferromagnetism, Phys. Rev. Lett. 126 (2021) 127701.

[18] Libor Šmejkal, Anna Birk Hellenes, Rafael González-Hernández, Jairo Sinova, Tomas Jungwirth, Giant and tunneling magnetoresistance in unconventional collinear antiferromagnets with nonrelativistic spin-momentum coupling, Phys. Rev. X 12 (2022) 011028.

[19] Xiaodong Zhou, Wanxiang Feng, Run-Wu Zhang, Libor Smejkal, Jairo Sinova, Yuriy Mokrousov, Yugui Yao, Crystal thermal transport in altermagnetic RuO2, 2023, arXiv:2305.01410[cond-mat.mtrl-sci].

[20] Jabir Ali Ouassou, Arne Brataas, Jacob Linder, Dc josephson effect in altermagnets, Phys. Rev. Lett. 131 (2023) 076003.

[21] Wojciech Brzezicki, Spin, orbital and topological order in models of strongly correlated electrons, J. Phys.: Condens. Matter 32 (2) (2019) 023001.

[22] Carmine Autieri, Biplab Sanyal, Unusual ferromagnetic YMnO3 phase in YMnO3/La2 / 3Sr1 / 3MnO3 heterostructures, New J. Phys. 16 (11) (2014) 113031.

[23] C. Autieri, M. Cuoco, G. Cuono, S. Picozzi, C. Noce, Orbital order and ferromagnetism in LaMn1−xGaxO3, Physica B 648 (2023) 414407.

[24] Carmine Autieri, Erik Koch, Eva Pavarini, Mechanism of structural phase transitions in $KCrF_3$, Phys. Rev. B 89 (2014) 155109.

[25] E. Gorelov, M. Karolak, T.O. Wehling, F. Lechermann, A.I. Lichtenstein, E. Pavarini, Nature of the mott transition in Ca_2RuO_4, Phys. Rev. Lett. 104 (2010) 226401.

[26] Nicolas Gauquelin, Filomena Forte, Daen Jannis, Rosalba Fittipaldi, Carmine Autieri, Giuseppe Cuono, Veronica Granata, Mariateresa Lettieri, Canio Noce, Fabio Miletto-Granozio, Antonio Vecchione, Johan Verbeeck, Mario Cuoco, Pattern formation by electric-field quench in a mott crystal, Nano Lett. http://dx.doi.org/10.1021/acs.nanolett.3c00574, PMID: 37200109.

[27] Davide Curcio, Charlotte E. Sanders, Alla Chikina, Henriette E. Lund, Marco Bianchi, Veronica Granata, Marco Cannavacciuolo, Giuseppe Cuono, Carmine Autieri, Filomena Forte, Alfonso Romano, Mario Cuoco, Pavel Dudin, Jose Avila, Craig Polley, Thiagarajan Balasubramanian, Rosalba Fittipaldi, Antonio Vecchione, Philip Hofmann, Current driven insulator-to-metal transition without mott breakdown in Ca_2RuO_4, 2023, arXiv:2303.00662[cond-mat.str-el].

[28] Wojciech Brzezicki, Filomena Forte, Canio Noce, Mario Cuoco, Andrzej M. Oleś, Spin-orbital mechanisms for negative thermal expansion in Ca_2RuO_4, Phys. Rev. B 107 (2023) 104403.

[29] C. Cirillo, V. Granata, G. Avallone, R. Fittipaldi, C. Attanasio, A. Avella, A. Vecchione, Emergence of a metallic metastable phase induced by electrical current in Ca_2RuO_4, Phys. Rev. B 100 (2019) 235142.

[30] M. De Raychaudhury, E. Pavarini, O.K. Andersen, Orbital fluctuations in the different phases of $LaVO_3$ and YVO_3, Phys. Rev. Lett. 99 (2007) 126402.

[31] Peter Horsch, Andrzej M. Oleś, Adolfo Avella, Orbital rotations induced by charges of polarons and defects in doped vanadates, Phys. Rev. B 103 (2021) 035129.

[32] Wojciech Brzezicki, Adolfo Avella, Mario Cuoco, Andrzej M. Oleś, Doped spin–orbital mott insulators: Orbital dilution versus spin–orbital polarons, J. Magn. Magn. Mater. 543 (2022) 168616.

[33] Adolfo Avella, Peter Horsch, Andrzej M. Oleś, Defect states and excitations in a mott insulator with orbital degrees of freedom: Mott-hubbard gap versus optical and transport gaps in doped systems, Phys. Rev. B 87 (2013) 045132.

[34] Adolfo Avella, Andrzej M. Oleś, Peter Horsch, Defect-induced orbital polarization and collapse of orbital order in doped vanadium perovskites, Phys. Rev. Lett. 122 (2019) 127206.

[35] Xue-Jing Zhang, Erik Koch, Eva Pavarini, $LaVO_3$: A true kugel-khomskii system, Phys. Rev. B 106 (2022) 115110, URL https://link.aps.org/doi/10.1103/PhysRevB.106.115110.

[36] G. Kresse, J. Hafner, Ab initio molecular dynamics for liquid metals, Phys. Rev. B 47 (1993) 558–561, URL https://link.aps.org/doi/10.1103/PhysRevB.47.558.

[37] G. Kresse, J. Furthmüller, Efficiency of ab-initio total energy calculations for metals and semiconductors using a plane-wave basis set, Comput. Mater. Sci. 6 (1) (1996) 15–50.

[38] G. Kresse, J. Furthmüller, Efficient iterative schemes for ab initio total-energy calculations using a plane-wave basis set, Phys. Rev. B 54 (1996) 11169–11186.

[39] John P. Perdew, Kieron Burke, Matthias Ernzerhof, Generalized gradient approximation made simple, Phys. Rev. Lett. 77 (1996) 3865–3868.

[40] C. Autieri, Antiferromagnetic and xy ferro-orbital order in insulating SrRuO3 thin films with SrO termination, J. Phys.: Condens. Matter 28 (42) (2016) 426004.

[41] Loïg Vaugier, Hong Jiang, Silke Biermann, Hubbard *U* and hund exchange *J* in transition metal oxides: Screening versus localization trends from constrained random phase approximation, Phys. Rev. B 86 (2012) 165105.

[42] C. Etz, I.V. Maznichenko, D. Böttcher, J. Henk, A.N. Yaresko, W. Hergert, I.I. Mazin, I. Mertig, A. Ernst, Indications of weak electronic correlations in $SrRuO_3$ from first-principles calculations, Phys. Rev. B 86 (2012) 064441.

[43] James M. Rondinelli, Nuala M. Caffrey, Stefano Sanvito, Nicola A. Spaldin, Electronic properties of bulk and thin film $SrRuO_3$: Search for the metal-insulator transition, Phys. Rev. B 78 (2008) 155107.

[44] Giuseppe Cuono, Carmine Autieri, Mott insulator Ca2RuO4 under external electric field, Materials 15 (19) (2022).

[45] Spriha Kumari, Sanhita Paul, Satyabrata Raj, Electronic structure of RVO3 (R=La and Y): Effect of electron (U) and exchange (J) correlations, Solid State Commun. 268 (2017) 20–25.

[46] M. Reehuis, C. Ulrich, P. Pattison, B. Ouladdiaf, M.C. Rheinstädter, M. Ohl, L.P. Regnault, M. Miyasaka, Y. Tokura, B. Keimer, Neutron diffraction study of YVO_3, $NdVO_3$, and $TbVO_3$, Phys. Rev. B 73 (2006) 094440.

[47] J.H. Jung, Z. Fang, J.P. He, Y. Kaneko, Y. Okimoto, Y. Tokura, Change of electronic structure in Ca_2RuO_4 induced by orbital ordering, Phys. Rev. Lett. 91 (2003) 056403.

[48] D. Sutter, C.G. Fatuzzo, S. Moser, M. Kim, R. Fittipaldi, A. Vecchione, V. Granata, Y. Sassa, F. Cossalter, G. Gatti, M. Grioni, H.M. Rønnow, N.C. Plumb, C.E. Matt, M. Shi, M. Hoesch, T.K. Kim, T-R Chang, H-T Jeng, C. Jozwiak, A. Bostwick, E. Rotenberg, A. Georges, T. Neupert, J. Chang, Hallmarks of hunds coupling in the mott insulator Ca2RuO4, Nature Commun. 8 (2017) 15176.

[49] E. Pavarini, I.I. Mazin, First-principles study of spin-orbit effects and NMR in Sr_2RuO_4, Phys. Rev. B 74 (2006) 035115.

[50] Carmine Autieri, Mario Cuoco, Canio Noce, Collective properties of eutectic ruthenates: Role of nanometric inclusions, Phys. Rev. B 85 (2012) 075126.

[51] D.J. Groenendijk, C. Autieri, T.C. van Thiel, W. Brzezicki, J.R. Hortensius, D. Afanasiev, N. Gauquelin, P. Barone, K.H.W. van den Bos, S. van Aert, J. Verbeeck, A. Filippetti, S. Picozzi, M. Cuoco, A.D. Caviglia, Berry phase engineering at oxide interfaces, Phys. Rev. Res. 2 (2020) 023404.

[52] T.C. van Thiel, W. Brzezicki, C. Autieri, J.R. Hortensius, D. Afanasiev, N. Gauquelin, D. Jannis, N. Janssen, D.J. Groenendijk, J. Fatermans, S. Van Aert, J. Verbeeck, M. Cuoco, A.D. Caviglia, Coupling charge and topological reconstructions at polar oxide interfaces, Phys. Rev. Lett. 127 (2021) 127202.

[53] Lin Yang, Lena Wysocki, Jörg Schöpf, Lei Jin, András Kovács, Felix Gunkel, Regina Dittmann, Paul H.M. van Loosdrecht, Ionela Lindfors-Vrejoiu, Origin of the hump anomalies in the hall resistance loops of ultrathin $SrRuO_3/SrIrO_3$ multilayers, Phys. Rev. Mater. 5 (2021) 014403.

[54] Gerald Malsch, Dmytro Ivaneyko, Peter Milde, Lena Wysocki, Lin Yang, Paul H.M. van Loosdrecht, Ionela Lindfors-Vrejoiu, Lukas M. Eng, Correlating the nanoscale structural, magnetic, and magneto-transport properties in SrRuO3-based perovskite thin films: Implications for oxide skyrmion devices, ACS Appl. Nano Mater. 3 (2020).

[55] Lena Wysocki, Jörg Schöpf, Michael Ziese, Lin Yang, András Kovács, Lei Jin, Rolf B. Versteeg, Andrea Bliesener, Felix Gunkel, Lior Kornblum, Regina Dittmann, Paul H.M. van Loosdrecht, Ionela Lindfors-Vrejoiu, Electronic inhomogeneity influence on the anomalous hall resistivity loops of SrRuO3 epitaxially interfaced with 5d perovskites, ACS Omega 5 (2020).

[56] Samuel V. Gallego, Emre S. Tasci, Gemma de la Flor, J. Manuel Perez-Mato, Mois I. Aroyo, Magnetic symmetry in the bilbao crystallographic server: a computer program to provide systematic absences of magnetic neutron diffraction, J. Appl. Crystallogr. 45 (6) (2012) 1236–1247.

[57] Lin-Ding Yuan, Alex Zunger, Degeneracy removal of spin bands in collinear antiferromagnets with non-interconvertible spin-structure motif pair, Adv. Mater. 35 (2023) 2211966.